CrystEngComm

Growth manner of rod-shaped ZnO crystals at low temperature without seed/buffer layer on polyimide film

Journal:	*CrystEngComm*
Manuscript ID	CE-ART-11-2020-001729.R1
Article Type:	Paper
Date Submitted by the Author:	17-Jan-2021
Complete List of Authors:	Shishino, Kazuyuki; Shinshu Daigaku; Toray Engineering Co., Ltd Yamada, Tetsuya; Shinshu Daigaku, Center for Energy and Environmental Science Fujisawa, Kazunori; Shinshu University, Faculty of Engineering Ikeda , Munekazu; Toray Engineering Co Ltd Hirata, Hajime; Toray Engineering Co Ltd Motoi, Masashi; Toray Engineering Co Ltd Hatakeyama, Tatsuo; Toray Engineering Co Ltd Teshima, Katsuya; Shinshu University, Department of Materials Chemistry; Shinshu University, Center for Energy and Environmental Science

ARTICLE

Growth manner of rod-shaped ZnO crystals at low temperature without seed/buffer layer on polyimide film

Received 00th January 20xx,
Accepted 00th January 20xx

DOI: 10.1039/x0xx00000x

Kazuyuki Shishino [ab], Tetsuya Yamada [c], Kazunori Fujisawa [c], Munekazu Ikeda [b], Hajime Hirata [b], Masashi Motoi [cd], Tatsuo Hatakeyama [ce], Katsuya Teshima [*cf]

ZnO is widely used as a semiconductor material in a variety of applications. Usually, ZnO is used as a thin film, which is composed of ZnO/intermediate layers/substrates. Recently we developed a rod-shaped ZnO crystal layer directly on a polyimide film without any intermediate layers by solution reaction coupled with surface treatments of the film. We studied the growth mechanism of ZnO crystal layers on the polyimide surface in the solution process. The physical and chemical effects of alkali, plasma, and heating treatments were clarified. The results indicated formation of homogenous, fine irregularities on the polyimide surface and predominance of imide groups. The direct growth of ZnO crystals is attributed to the anchor effect derived from gradual nuclear growth of $Zn(OH)_2$ in the homogeneous, fine irregularities of the polyimide film. We also demonstrated a more facile approach for the preparation of ZnO crystal layers by physical roughening of the polyimide film to verify our proposed mechanism. Our findings provide new insights for the growth of ZnO crystals on polyimide and other polymer substrate surfaces without the use of any intermediate layer. This knowledge may be further used for mass production of ZnO crystal/polyimide thin films at low cost.

1. Introduction

ZnO is a wurtzite type anisotropic oxide material which can be prepared at low temperature (< 100 °C) and low cost.[1–2]. ZnO exhibits various features, including transparency, semiconductor properties, and flexible crystal shapes.[3] These characteristics make ZnO a promising material for transparent electrodes, vibration sensors, biosensors, white light-emitting diodes, and so on.[4–7] Various studies have been reported on the film formation of ZnO crystals. Usually, an intermediate oxide (ZnO, Al_2O_3, etc.) or metal (Au, Cr, etc.) layer is used as a seed or buffer layer to grow ZnO crystals on a substrate.[8–11] The deposition of these intermediates makes the fabrication process of ZnO thin films complicated and expensive and also upsizes devices. Recently, we deposited rod-shaped ZnO crystal layer directly on a polyimide film without using any intermediate layers.[12] This was achieved through aqueous solution reaction of ZnO crystals coupled with surface treatment of the polyimide film using alkali, plasma, and heating (3-step process). In another study, aerosol approach was used to deposit rod-shaped ZnO crystals directly on a silicon substrate at 400–500 °C. [13–14] However, this method cannot be applied to general resin materials of low thermal stability.

Although our ZnO crystal/polyimide film has the advantage of using no intermediate layer, its mass production is limited by the following factors. Firstly, this method requires large-scale infrastructure because of complicated processes under vacuum atmosphere and use of large amount of solution. These issues make it unsuitable for mass production using typical methods such as single wafer processing and roll-to-roll manufacturing, because the number of processes and the convenience of each step are directly linked to the production efficiency in terms of time and cost. Secondly, substrates other than polyimide have not been used for direct deposition of ZnO crystal. Polyimide is a flexible, workable, and lightweight resin material which exhibits moderately high thermal and solvent resistances, thus imparting various functional properties as substrates.[15] However, polyimide is an insulator, and its function is limited. Considering the extensive applications of ZnO, it is essential to use other substrates, including polymer and two-dimensional semiconductor materials, for direct deposition. For example, ZnO can enhance optical, electrical, and optoelectronic properties when combined with graphene and transition metal dichalcogenides.[16-19]

Simplification of the fabrication process and use of other polymer substrates are important for scaling up our suggested ZnO thin film deposition method. To realize them, it is necessary to understand the

[a] Graduate School of Medicine, Science and Technology, Shinshu University, 4-17-1 Wakasato, Nagano 380-8553, Japan
[b] Research & Development Div, Toray Engineering Co., Ltd., 1-1, Sonoyama 1-chome, Otsu, Shiga, Japan.
[c] Research Initiative for Supra-Materials, Shinshu University, 4-17-1 Wakasato, Nagano 380-8553, Japan.
[d] Development Team, Business Div. Ⅱ, Mechatronics & Fine Technology Business Div, Toray Engineering Co., Ltd., 1-45, Oe 1-chome, Otsu, Shiga, Japan
[e] Development Team, Business Div. Ⅰ, Mechatronics & Fine Technology Business Div, Toray Engineering Co., Ltd., 1-45, Oe 1-chome, Otsu, Shiga, Japan
[f] Department of Materials Chemistry, Faculty of Engineering, Shinshu University, 4-17-1 Wakasato, Nagano 380-8553, Japan
* Corresponding author's email: teshima@shinshu-u.ac.jp

†Electronic Supplementary Information (ESI) available: Line-scan surface roughness of the polyimide film of (a) initial state and (b) alkaline, (c) plasma, (d) heat, and (e) 3-step process treatments. (ESI.1). White light interferometer images of the polyimide film polished by (a) 400#, (b) 2000#, (c) 20000#. (ESI.2). Line-scan surface roughness of the polyimide film polished by sandpapers of grade (a) 400 #, (b) 2000 #, (c) 20000 #.(ESI.3).FT-IR spectra of the polyimide film after polishing treatment using grain size of (a)400#, (b)2000#, and (c)20000# in red color. FT-IR spectrum of the non-treated film is shown in black color in each figure. (ESI.4). See

mechanism for direct growth of ZnO crystal layers on the polyimide surface. In our previous report, it was suggested that polyimide surface has irregularities which induce an anchor effect. However, the driving force for this effect has not been clarified, and the interfacial bonding state between ZnO crystal layers and polyimide is not fully understood.

Herein, we investigated the nucleation timing of Zn species on the polyimide film and the effect of the 3-step surface treatment process on the adhesion of ZnO crystal layer from the chemical and physical viewpoints. These results were used to propose a mechanism for direct growth of ZnO crystal layers on polyimide surface. We also prepared ZnO crystal layers/polyimide film using an alternate surface treatment approach to confirm the proposed growth mechanism.

2. Experimental

2.1 Deposition of ZnO crystal layers on the polyimide film

All the reagents were used without any purification. Polyimide film (Kapton® Type VN Film, DU PONT-TORAY CO., LTD.) was used as the substrate. After the chemical treatment steps in 2.1.1, The polyimide film was subjected to the following steps: washing with pure water, blowing off the water, and then drying in an oven at 60 °C for 15 min. ZnO crystal layer was grown after surface treatments of the polyimide film, as mentioned below.

2.1.1 Surface treatment of the polyimide film

The surface treatment of the polyimide film was carried out using alkali, plasma, heat (chemical treatment), and sandpaper (physical treatment).

I: Alkali treatment

The polyimide film was immersed in a mixed aqueous solution of 12 g/L $KMnO_4$ (99 %, Kanto Chemical Co., Inc.) and 4 g/L NaOH (95 %, Kanto Chemical Co., Inc.) at 80 °C for 5 min. For neutralization, the immersed film was placed in an aqueous solution of 7 g/L hydroxylamine hydrochloride (96 %, Kanto Chemical Co., Inc.) at 40 °C for 1 min, and then in H_2SO_4 (98 %, MC FERTICOM Co., Ltd.) solution at 40 °C for 2 min.

II: Plasma treatment

The plasma treatment (SAMCO Inc, PC-1000) was performed at 500 W for 300 s under vacuum condition at 10 Pa and at around 25 °C. The vacuum was created by exhausting air and replacing with Ar several times.

III: Heating treatment

The heat treatment was performed at 400 °C for 3 h in total, including heating and holding processes. After the heat treatment, the film was naturally cooled down to room temperature.

IV: Polishing treatment

Three grades of sandpaper were used for polishing: 400#, 2000#, and 20000# (Trusco Nakayama Co., Ltd.). After slightly wetting the polyimide film with pure water, rasping was carried out in the vertical, parallel, clockwise, and counterclockwise directions of the file for 2 min each. Subsequently, the polyimide film was wiped with a paper towel soaked with liquid in the order of pure water and ethanol to remove the polishing powder.

2.1.2 Deposition of ZnO crystal layers

We grew ZnO crystal layer directly on the polyimide film without seed/ buffer layer by using the solution method reported in our previous study. First, 44.57 g (30 mM) $Zn(NO_3)_2 \cdot 6H_2O$ (99%, Alfa Aesar.com) was added into 5 L water at 50 °C and stirred for 5 min. Then, 21.13 g (30 mM) hexamethylenetetramine (HMT) (99%, Fuji Film Wako Pure Chemical Industries, Ltd.) was added and further mixed for 5 min. No apparent change was observed at this point. The surface-treated polyimide film was immersed in this solution for 1 h. Then, the reactants were heated up to an arbitrary temperature between 50 and 90 °C. The total time between the first immersion of the film and the end of heating was 3 h. After cooling, the film was taken out and washed with warm water (70 °C) for 1 min. Next, the water was blown off, and the film was dried in an oven at 60 °C for 15 min.

Table 1 summarizes the experimental conditions used for preparing ZnO crystals on polyimide. The numbers in the "Surface treatment" columns indicate the order of treatment. The numbers in "Polishing" indicates the grade of sandpaper. Heating was performed in two steps, which is denoted as "1st step" and "2nd step" in "Preparation of ZnO". The heating temperature and heating time are denoted as "Temp./ °C" and "Time/ h", respectively. Process no. 8 corresponds to the experimental condition used in our previous study,[12] which was repeated in this study for comparison.

Table 1 Experimental conditions used for the deposition of ZnO crystal layers on the polyimide film.

Process no.	Surface treatment of the polyimide film				Preparation of ZnO			
					1st step		2nd step	
	Alkali	Plasma	Heat	Polishing	Temp. / °C	Time / h	Temp. / °C	Time / h
1	-	-	-	-	50	2	-	-
2	-	-	-	-	50	1	90	1
3	-	-	-	-	90	2	-	-
4	-	-	-	-	50	1	90	2
5	1				50	1	90	2
6	-	1	-	-	50	1	90	2
7	-	-	1	-	50	1	90	2
8	1	2	3	-	50	1	90	2
9	1	3	2	-	50	1	90	2
10	-	-	-	400#	50	1	90	2
11	-	-	-	2000#	50	1	90	2
12	-	-	-	20000#	50	1	90	2

2.2 Characterization

The surface morphologies of the polyimide film were observed using a field emission scanning electron microscope (FESEM; JEOL Ltd., JSM-7600F). The sample was analyzed at an acceleration voltage of 15 kV after deposition Pt by electron sputtering. The structure was examined using X-ray diffraction (XRD; Rigaku Corporation, Miniflex600). The measurements were performed with Cu Kα radiation (λ = 0.154 nm) in the 2θ region between 10 and 80° at a scan speed of 10°·min^{-1} and a resolution of 0.02°. The chemical bonding state was investigated by Fourier transform infrared absorption (FT-IR; JASCO corporation: FT/IR6100) spectroscopy. The attenuated total reflection method was used for the measurement. In the wavelength range of 500 to 4000 cm^{-1}, the measurement was performed at 4 cm^{-1} intervals and 100 times of integration. The surface roughness was measured using a three-dimensional white light interference microscope (Bruker Japan K.K: Contour GT-K0). Using a fiftyfold lens, measurement was performed within ±10 μm in the vertical direction from the surface to be measured.

The wettability of the surface-treated polyimide film was evaluated using a contact angle measuring device (Kyowa Interface Science Co., Ltd.: DMo-701). The 2θ method was used for the calculation of the contact angle, and the measurement was performed 10 times per one level. To reduce the influence of gravity, the water droplet size was set to 1.5 μL. The coverage of the ZnO crystal layer for the polyimide film was analyzed using image processing software (Toray Engineering Co., Ltd.: InkJetObserveStd). Using the image data obtained by SEM measurements, the thresholds of ZnO (white part of the image) and polyimide film (black part of the image) were set to 100, and the ratio of the white pixel area and the black pixel area was calculated.

Crystallographic characteristics were evaluated by transmission electron microscopy (TEM, JEM-2100F (JEOL) equipped with CESCOR and CETCOR (CEOS)), at an acceleration voltage of 80 kV. In order to transfer grown rod-like ZnO crystals on the polyimide substrate, the surface of the substrate was first scratched by spatula, and then a Cu TEM grid was placed over the scratched surface of ZnO/polyimide. Detached ZnO was transferred by dropping a drop of ethanol over TEM grid/ZnO/polyimide, followed by natural drying.

The adhesion between the ZnO crystal layer and the polyimide film was evaluated by performing a peel test. The ZnO crystal layer/polyimide film was fixed on a peeling machine (MinebeaMitsumi Inc., LTS-500N), and a tape (Nichiban Co., Ltd: NW25) with width and length of 20 mm was attached to the surface of the ZnO crystal layer. The load was measured using a load cell while pulling the tape at an angle of 90° from the sample at 20 mm/min until the tape peeled off from the sample.

3. Result and Discussion

To understand the direct growth of ZnO crystal on polyimide film, we examined the nucleation timing of Zn species on the polyimide film and the effects of the chemical and physical surface treatments on the film properties.

3.1 Nucleation timing and growth of ZnO on polyimide

The nucleation of reactants on the polyimide film is important for constructing strong interfacial bonding between polyimide and ZnO. So, we investigated the formation process of ZnO in solution. After setting the reaction solution at each temperature of 50, 70, and 90 °C, the solid contents generated in the solution were analyzed. The XRD patterns of the solid contents are shown in Fig. 1. The patterns were compared with the reference data of Crystallography Open Database (COD) to identify the composition. At 50 °C, the main phase is $Zn(OH)_2$ with ZnO as the subphase. At 70 °C and above, only peaks corresponding to ZnO are observed, indicating that $Zn(OH)_2$ is dehydrated to ZnO at a temperature of 70 °C or higher.

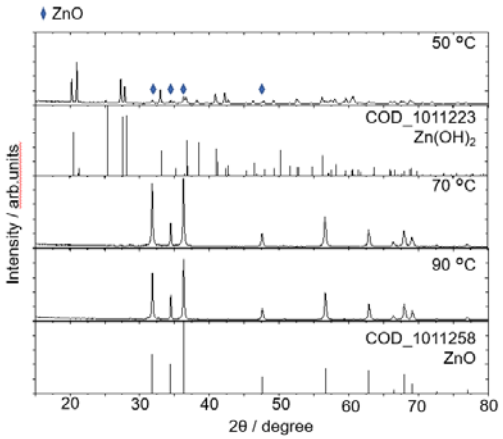

Fig.1 XRD patterns of the solid contents formed from the mixed solution of $Zn(NO_3)_2$ and HMT after heating at 50, 70, and 90 °C. The XRD patterns of standard $Zn(OH)_2$ (COD_1011223) and ZnO (COD_1011258) are also shown for reference.

Figure 2 shows the SEM images of the solid contents. The product obtained at 50 °C consists of amorphous secondary particles of size less than 10 μm, as shown in Fig. 2(a). As shown in the inset, the primary particle is irregular in shape with size of approximately 0.1 μm. The product obtained at 70 °C consists of aggregates, and the primary particles are rod-shaped crystals

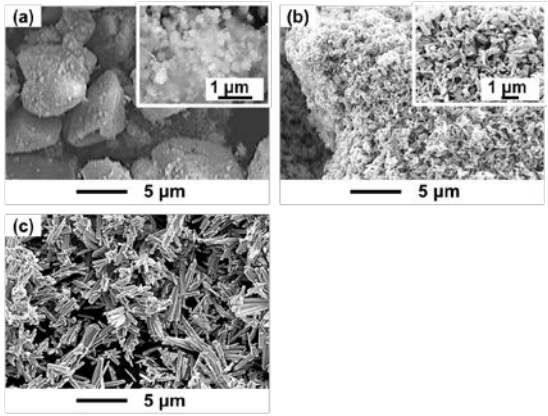

Fig.2 SEM images of the solid contents formed from the mixed solution of $Zn(NO_3)_2$ and HMT after heating at (a) 50, (b) 70, and (c) 90 °C.

with length less than 1 µm, as shown in Fig. 2(b). At 90 °C, no aggregation is observed, and rod-shaped crystals with length of approximately 5 µm are formed, as shown in Fig. 2(c). Comparing with the XRD results, it can be inferred that the Zn species in the solution correspond to amorphous secondary particles of $Zn(OH)_2$ at low temperature, which transform to rod-shaped crystals of ZnO after heating.

To identify the first adhesion of ZnO species with the polyimide film in the solution, the effect of heating/holding temperature on the adhesion was examined. A non-treated polyimide film was immersed in a mixed solution of $Zn(NO_3)_2$ and HMT and heated under three different conditions (process nos. 1–3, also see Fig. 3(a)). Figure 3(b) shows the SEM image of the polyimide film immersed at 50 °C for 2 h (process no. 1). Fine crystals of size less than 1 µm cover the entire polyimide film. From the image analysis, the coverage was estimated to be approximately 87%. When the polyimide film was immersed at 50 °C for 1 h, followed by holding at 90 °C for 1 h (process no. 2), the adhered particles became large, and the coverage deteriorated to 76% with low uniformity (Fig. 3(c)). When the heating process was drastically changed to 90 °C for 2 h (process no. 3), the coverage further decreased to 47% (Fig. 3(d)). These results suggest that the nucleation of $Zn(OH)_2$ on the polyimide film is related to the interfacial bonding between ZnO and polyimide.

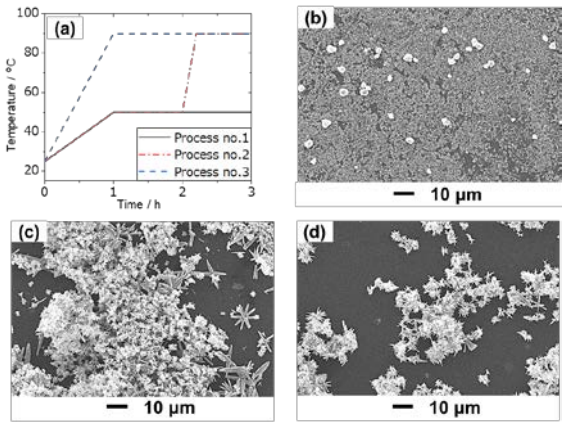

Fig.3 (a) Temperature profiles of process nos. 1–3. SEM images of the reactants on the non-treated polyimide film after immersing in the mixed solution of $Zn(NO_3)_2$ and HMT at (b) 50 °C for 2 h (process no. 1), (c) 50 °C for 1 h, then 90 °C for 1 h (process no. 2), and (d) 90 °C for 2 h (process no. 3).

3.2 Physical and chemical effects of the surface treatment

The interfacial bonding between ZnO and the polyimide film was examined by analyzing the effect of each surface treatment on the polyimide film by three-dimensional white light interference microscopy and spectroscopy. Figure 4(a) shows the microscopic image of the non-treated polyimide surface in the range of about 48 µm × 36 µm. We evaluated the surface roughness in terms of Rz_{JIS}, which is the average value of 10 points of the difference between the location with the largest convex portion, the position of its skirt, and its surroundings. The surface roughness the non-treated polyimide film was estimated to be 0.01 µm, and the spacing between the surface irregularities was more than 5 µm. The microscopic images of the polyimide surface after alkali treatment (Fig. 4(b)), plasma treatment (Fig. 4(c)), and heat treatment (Fig. 4(d)) are also shown. The alkali-treated polyimide film shows a higher surface roughness of approximately 0.18 µm, while the surface roughnesses of the plasma-treated and the heat-treated polyimide films are similar to that of the non-treated polyimide film. Figure 4(e) shows the microscopic image of the 3-step (alkali, plasma, and heat) surface-treated polyimide. The surface roughness is 0.09 µm and the spacing between the irregularities is less than 1 µm, which is smaller than that of the alkali-treated film. The surface roughness values (Rz_{JIS}) are summarized in Table 2. Figure S1 also shows line-scan roughness of each surface-treated film.

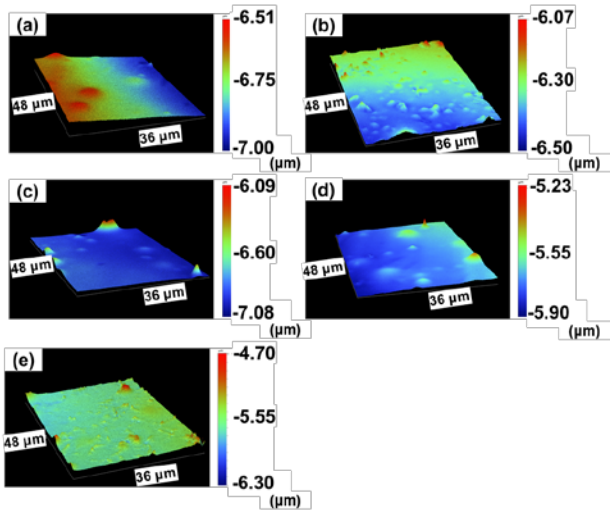

Fig.4 (a) White light interference microscope images of (a) non-treated polyimide film and polyimide film subjected to (b) alkali, (c) plasma, (d) heating, and (e) 3-step process treatments.

Table 2 Surface roughness of the polyimide film in the non-treated state and after each surface treatment.

Unit: µm	non-treated	alkali	plasma	heating	3-step process
surface roughness	0.01	0.18	0.03	0.02	0.09

The local chemical state of each polyimide film was determined using FT-IR, and the results are shown in Figure 5. The black and the red curves indicate the spectra of non-treated polyimide film and polyimide film after each surface treatment, respectively. It has been reported that polyimide exhibits three intrinsic peaks: C=O stretch vibration (1720 cm^{-1}) derived from imide, C-N stretch vibration (1370 cm^{-1}) and C=C stretch vibration (1500 cm^{-1}) derived from the aromatic ring.[20]. As the C=C stretch (int A) hardly changes in the chemical state, we evaluated the intensity ratio of C=O stretch (int B/ int A) and C–N stretch (int C/ int A), as shown in Table 3. After alkaline

treatment, the int B/ int A and int C/ int A values were 0.79 and 1.22, respectively which are close to the values of non-treated polyimide (int B/ int A = 0.81 and int C/ int A = 1.20). We also confirmed hydrophilization of the alkaline treated polyimide as compared with non-treated polyimide by visual observation of contact angle of water droplets. It has been reported that a part of the imide bond of polyimide is cleaved by alkali treatment to generate a carboxyl group, which increases the hydrophilicity.[21] From these results, we concluded that carboxyl group was generated on the polyimide surface by the alkali treatment, though the change could not be observed by FT-IR. Plasma treatment resulted in int B/ int A and int C/ int A values of 0.73 and 1.27, respectively. Considering that the intensity ratio is calculated from the transmittance, this result suggests an increase in the C=O stretch mode and a decrease in the C–N stretch mode. The imide group of the polyimide is easily cleaved by the plasma treatment to generate a carboxyl group and amidate.[22] Similar changes might occur on the surface and inside the bulk of the polyimide. In contrast to the plasma treatment, the int B/ int A and int C/ int A values after heat treatment were 0.89 and 1.10, respectively. This is attributed to an increase in the imide groups because of the dehydration condensation of the carboxyl group and the amide group in polyimide, as reported in reference.[23] In the case of the 3-step process, the int B/ int A and int C/ int A values were 0.81 and 1.20, respectively which are similar to those of the non-treated polyimide. This result is attributed to cleavage/ reconstruction of the imide group.

The surface treated polyimide films were further tested for adhesion of the ZnO crystal layer after heating in the solution. Figure 6 shows the SEM images of the reactants. When the non-treated polyimide film was used (process no. 4), some amount of ZnO adhered to the film as shown in Fig. 6(a). By binarizing the SEM image, the coverage of the ZnO crystals on the

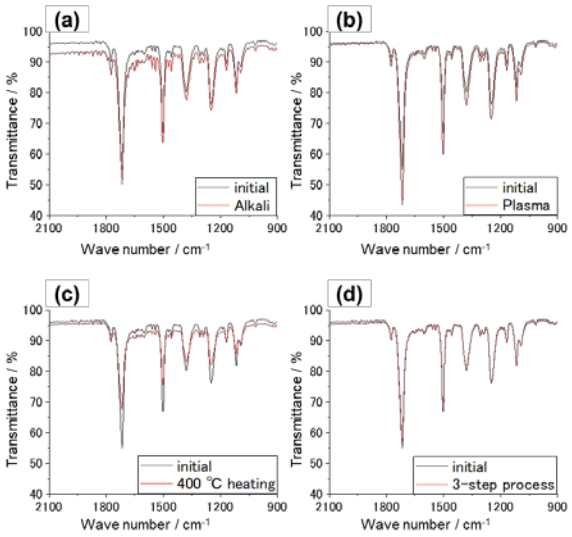

Fig.5 FT-IR spectra of the polyimide film after treatment (red color) with (a) alkali, (b) plasma, (c) heat, and (d) 3-step process. The FT-IR spectrum of the non-treated polyimide film is shown in black color in each figure.

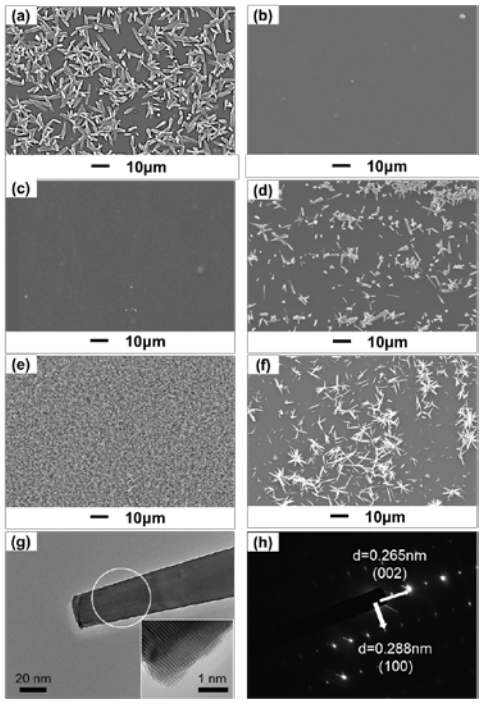

Fig.6 SEM images of the reactants after formation of ZnO in the solution while using (a) non-treated polyimide film (process no. 4); and polyimide films chemically treated by (b) alkali (process no. 5), (c) plasma (process no. 6), (d) heat (process no. 7), (e) 3-step process (alkali, plasma, then heat; process no. 8), and (f) alternate 3-step process (alkali, heat, then plasma; process no. 9). (g) HR-TEM images of the rod-like ZnO crystal in Fig. 6(e). (h) SAED pattern obtained from the circular area in (g)

Table 3 Spectral information obtained from the FT-IR measurements of polyimide film after the chemical surface treatments.

Surface treatment	Peak intensity at each specific vibration mode			Peak intensity ratio of C=O and C=C	Peak intensity ratio of C–N and C=C
	Int A C=C stretch at 1500 cm^{-1}	*Int B* C=O stretch at 1720 cm^{-1}	*Int C* C–N stretch at 1370 cm^{-1}	*Int B/ Int A*	*Int C/ Int A*
Non-treated	66.9	54.33	80.31	0.81	1.20
Alkali	63.94	50.40	77.71	0.79	1.22
Plasma	59.96	43.80	76.01	0.73	1.27
Heat	75.79	67.52	83.21	0.89	1.10
3-step	67.99	57.25	80.74	0.81	1.20

polyimide film was estimated to be approximately 52%. No crystal adhesion was observed in the cases of alkali- (process no. 5) and plasma- (process no .6) treated polyimide films [Figs. 6(b) and (c)]. When the heat-treated (process no. 7) film was used, little amount of crystal adhesion was observed (Fig. 6(d)). The coverage was estimated to be 21%, which is less than half of the adhesion obtained using non-treated polyimide. Surface treatment by the 3-step process (process no. 8) resulted in complete coverage of the polyimide film with ZnO crystals as evident in Fig. 6(e), which is the best among all the process conditions. It is also notable that the surface treatments affected the size of ZnO crystals (see Figs. 6(a) and (e)). When the order of plasma and heating was changed in the 3-step process (Fig. 6(f), process no. 9), the coverage decreased to approximately 45%. In this case, the adhesion rate decreased, suggesting that the plasma treatment is inevitable for improving the adhesion and its order in the processes is important. We also carried out TEM observation of the rod-like ZnO crystals in Figure 6(e). The high-resolution TEM (HR-TEM) image in Figure 6(g) shows a single domain ZnO with no clear grain boundaries. Moreover, higher magnification HR-TEM image (the inset) exhibits uniform lattice fringes over the entire crystal with no atomic defects, which indicates that the crystallinity of grown ZnO is high. The selected area electron diffraction (SAED) pattern obtained from the circular area in Figure 6(g) reveals periodically ordered diffraction spots, as shown in Figure 6(h). From this pattern, we found that the growth direction of the long axis accords to <001>. It has already been known that ZnO crystals easily grow in the <001> direction.[24] Therefore, we conclude that no apparent influence that determines the growth direction of ZnO crystals exists at the polyimide surface. It is considered that the contact among ZnO-polyimide is dominantly affected by anchor effect as physical effect, rather than the chemical effect.

3.3 Peel test

The interfacial bonding strength of ZnO crystal and the 3-step surface-treated polyimide films was examined by performing a peel test. Figure 7(a) shows the relationship between the peel strength and the peel distance. As the pull distance was increased, the peel strength increased to a maximum and then

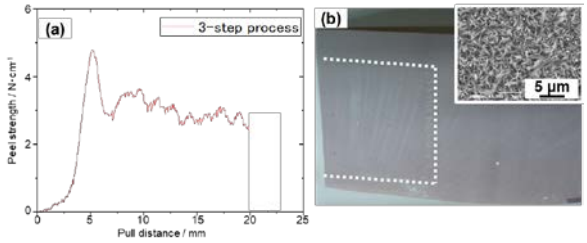

Fig.7 (a) Peel-test results for ZnO layer deposited on the polyimide film treated by the 3-step process (process no. 8). (b) Photograph and SEM image (inset) of the ZnO layer after the peel test. The dashed lines in white indicate the peel testing area.

decreased with slight oscillations. The test was terminated when the peel distance reached 20 mm. The sample exhibited a maximum tensile strength of 5 $N \cdot cm^{-1}$ and exhibited a tensile strength of 2 $N \cdot cm^{-1}$ at 20 mm. Figure 7(b) shows the photograph and the SEM image of the sample after the peel test. No apparent change is observed on the adhered crystals after peeling (compared to Fig. 6(e)). This result indicates strong interfacial bonding between ZnO and the polyimide film.

3.4 Mechanism for formation of rod-shaped ZnO crystals

From the observations of nucleation of Zn species on the polyimide film and the effects of surface treatments, we propose the following mechanism for direct growth of ZnO crystal layer on the polyimide film; the schematic representation is shown in Fig. 8.

Step 1: Surface treatments

In the first step, the alkali treatment produced sparse irregularities on the surface of the polyimide film. The alkali treatment also caused formation of carboxyl group through imide cleavage. In the second step, the surface irregularities formed by the alkali treatment were flattened and densified by

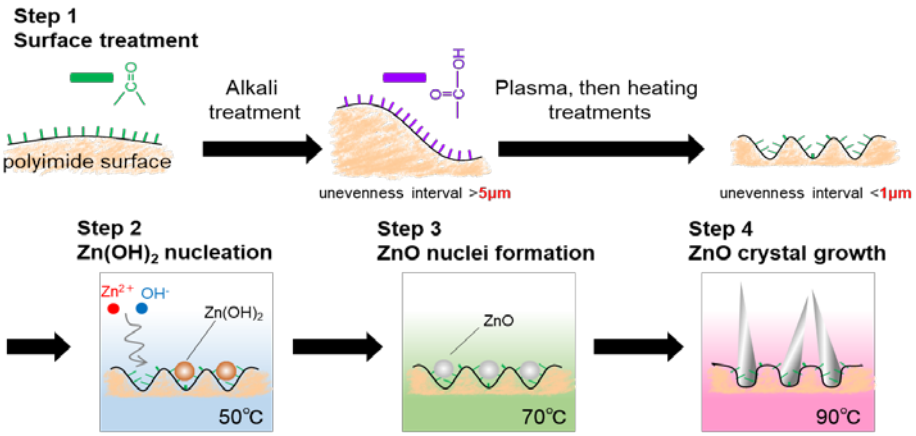

Fig.8 Schematic representation of the effect of surface treatments of the polyimide film and subsequent formation of ZnO crystal layers directly on the film in solution.

the subsequent plasma treatment. It has been reported that plasma treatment results in fine surface irregularities of approximately 10 nm on a polyimide film.[22] Simultaneously the imide group was cleaved to carboxyl group in the bulk of the film by the plasma treatment, while heating led to recovery of imide groups on the surface and the inside of the polyimide film. Consequently, the surface of the polyimide film exhibited fine roughness with height of 0.09 μm, the spacing between the irregularities was reduced to less than 1 μm, and abundant imide groups (few carboxyl groups) existed on the surface of the polyimide film.

Step 2: $Zn(OH)_2$ nucleation

When $Zn(NO_3)_2$ and HMT were added to the aqueous solution at 50 °C, they immediately ionized according to the following reactions (Formulae 1 and 2).[25]

$Zn(NO_3)_2 \cdot 6H_2O \rightarrow Zn^{2+} + NO_3^{2-}$ (Formula 1)
$C_6H_{12}N_4 \rightarrow 6HCHO + 4NH_3$ (Formula 2-1)
$NH_3 + H_2O \rightarrow NH^{4+} + OH^-$ (Formula 2-2)

The Zn^{2+} and OH^- ions transported nearby the polyimide surface might interact with the imide group during its reaction to form insoluble $Zn(OH)_2$ (Formula 3).
$Zn^{2+} + 2OH^- \rightarrow Zn(OH)_2$ (Formula 3)
The $Zn(OH)_2$ nuclei interacted with the imide groups on the fine surface of the polyimide. The degree of surface roughness is expected to affect the adsorption efficiency of Zn species. This is because the contact area of Zn species with the polyimide surface depends on its roughness. In this case, the adsorption efficiency of Zn species increases on a suitable uneven surface, resulting in inhomogeneous nucleation on the entire surface of polyimide. We also found that ZnO crystals hardly adhered to the carboxyl group-rich polyimide surface. This may be because, in the present solution of abundant OH ions, $Zn(OH)_2$ likely changed to $Zn(OH)_4^{2-}$ and carboxyl group existed as COO^-, resulting in electric repulsion between them.[26]

Step 3: Formation of ZnO nuclei

As the solution temperature was increased, the $Zn(OH)_2$ nuclei on the surface of the polyimide film underwent a dehydration reaction to form ZnO nuclei (Formula 4) while keeping contact with the polyimide.

$Zn(OH)_2 \rightarrow ZnO + H_2O$ (Formula 4)

Step 4: ZnO crystal growth

With continuous supply of Zn from the solution, ZnO nuclei grew at the concave portion of the polyimide surface promoting the anchor effect. The direction of crystal growth was restricted by the recess of the polyimide surface, and the rod-like crystal shape was formed mostly perpendicular to the polyimide surface, as reported in our previous study.[12] The ZnO crystals obtained on the 3-step-treated polyimide surface was different in size and growth orientation from that obtained on the non-treated surface. We speculate that the surface roughness influenced the nucleation frequency of $Zn(OH)_2$, which also affected the crystal growth orientation and growth rate.

3.5 Demonstration of the proposed mechanism for direct formation of ZnO on the polyimide film

To confirm the proposed mechanism, we verified the ZnO crystal layer formation through an alternative approach. Instead of the 3-step surface treatment, we physically created roughness on the non-treated polyimide surface by sandpaper polishing. Subsequently, ZnO crystal layers were grown by dipping the film in the same solution. ESI 2(a) shows the three-dimensional white light interference microscope image of 400# sanded polyimide film. The surface roughness was approximately 1.48 μm, which is higher than the roughness obtained by chemical treatments. The surface roughness reduced with increase in the sandpaper grade: 0.11 μm for 2000# (ESI 2(b)) and 0.01 μm for 20000# (ESI 2(c)). The line-scan roughness of each surface-treated film is summarized in Figure S3. We also recorded the FT-IR spectra and found no significant change between the non-treated and the physically roughened sample in every case (ESI 4). Therefore, it can be concluded that no chemical change has occurred in the polyimide film.

Figure 9 shows the SEM images of the polyimide surface after the ZnO formation reaction in the solution. The crystals cover the entire surface of the film (100% coverage), as shown in Fig. 9(a), when 400# sanded film was used. The inset in the figure is an enlarged view which shows primary particles of the rod-shaped crystals with length of approximately 3 μm, similar to those obtained using the 3-step surface treatment (process no. 8).[11]. The rod-like crystals were also formed on the films polished using other sandpaper grades; however, their coverage decreased to 42% for 2000# (Fig. 9(b)) and 52% for 20000# sanded films (Fig. 9(c)). They show no significant difference compared with the ZnO growth on the non-treated film shown in Fig. 6(a). However, the size of the crystals decreased considerably with decrease in the grade of the sandpaper. Simultaneously, polishing accuracy affects the adhesion rate of ZnO crystals, which may be attributed to the degree of roughness depth and the spacing between the surface irregularities.

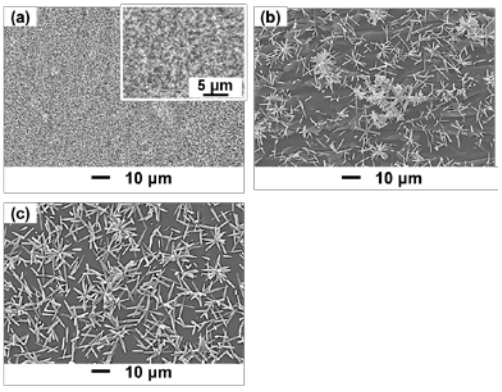

Fig.9 SEM images of the crystal reactants on the polyimide film polished by sandpapers of grade (a) 400# (process no. 10), (b) 2000# (process no. 11), and (c) 20000# (process no. 12).

As shown in the microscopic image of the polyimide surface, the polishing treatments resulted in irregularities of various depths and intervals. In the reaction field of the heated solution, the convecting Zn source should be effectively adsorbed onto the rough polyimide surface, similar to the surface obtained by polishing with 400# sandpaper. It is remarkable that direct adhesion of ZnO crystals on the polyimide film can be achieved with only physical treatment, instead of complicated chemical processes. Hence, it may be possible to improve the interfacial bonding between ZnO and other polymer substrates by designing the surface roughness more precisely. Furthermore, the orientation of the crystal itself may be controlled.

Conclusions

The growth mechanism of ZnO rod-shaped crystals directly on a polyimide film without deposition of any intermediate layer was investigated. At first, we examined the adhesion timing of Zn-based nuclei on polyimide in solution reaction in terms of chemical reaction in solution and immersion of polyimide film. During heating in solution, $Zn(OH)_2$ nuclei were formed which covered the polyimide surface completely, followed by formation of ZnO crystals while maintaining the contact. This indicates the contribution of $Zn(OH)_2$ nucleation for good adhesion. By microscopy and local structural analyses, the physical and chemical effects of alkali, plasma, and heating treatments were clarified. Combining them in this order, imide groups predominated on the polyimide surface and homogeneous, fine irregularities are formed. From these results, we deduced that the direct growth of ZnO crystals is due to the anchor effect derived from gradual nuclear growth of $Zn(OH)_2$ in the homogeneous, fine irregularities of the polyimide. We also carried out an alternate surface treatment approach using sandpaper to verify our proposed mechanism and found that similar ZnO adhesion occurred on the physically treated rough polyimide surface.

Our findings provide new insights for the preparation of ZnO/polyimide films without any intermediate layer. By fine tuning the surface roughness of the polyimide film, the adhesion strength can be improved for practical applications. Facile mass production of ZnO including roll-to-roll process will also be possible in future using this method. The proposed mechanism is also applicable to ZnO/polymer substrates, since the interfacial bonding between ZnO and the polyimide surface is not intrinsic to the material. In our future work, we plan to apply our fabrication technique to other substrates for flexible designs of ZnO thin film.

Conflicts of interest

The authors declare no competing financial interest.

Acknowledgements

This work was partially supported by JST Program on Open Innovation Platform with Enterprises, Research Institute and Academia JPMJOP1843, and JST Center of Innovation, Young Collaborative Research Fund, Digital Field R1WD12.

Notes and references

1. X. Wu, L. Zheng, D. Wu, Fabrication of Superhydrophobic Surfaces from Microstructured ZnO-Based Surfaces via a Wet-Chemical Route. *Langmuir*, 2005, **21**, 2665-2667.
2. D. Pradhan, K. T. Leung, Vertical Growth of Two-Dimensional Zinc Oxide Nanostructures on ITO-Coated Glass: Effects of Deposition Temperature and Deposition Time. *J. Phys. Chem. C,* 2008, **112**, 1357-1364.
3. S. Kumar, H. J. Lee, T. H. Yoon, C. N. Murthy, J. S. Lee, Morphological Control over ZnO Nanostructures from Self-Emulsion Polymerization. *Cryst. Growth Des.,* 2016, **16**, 3905−3911.
4. D. S. Bhachu, G. Sankar, I. P. Parkin, Aerosol Assisted Chemical Vapor Deposition of Transparent Conductive Zinc Oxide Films. *Chem. Mater.,* 2012, **24**, 4704-4710.
5. S. Joshi, M. M. Nayak, K. Rajanna, Evaluation of Transverse Piezoelectric Coefficient of ZnO Thin Films Deposited on Different Flexible Substrates: A Comparative Study on the Vibration Sensing Performance. *ACS Appl. Mater. Interfaces,* 2014, **6**, 7108−7116.
6. M. Ryu, J. H. Yang, Y. Ahn, M. Sim, K. H. Lee, K. Kim, T. Lee, S. J. Yoo, S. Y. Kim, C. Moon, M. Je, J. W. Choi, Y. Lee, J. E. Jang, Enhancement of Interface Characteristics of Neural Probe Based on Graphene, ZnO Nanowires, and Conducting Polymer PEDOT. *ACS Appl. Mater. Interfaces,* 2017, **9**, 10577−10586.
7. O. H. Kwon, J. W. Jang, S. J. Park, J. S. Kim, S. J. Hong, Y. S. Jung, H. Yang, Y. J. Kim, Y. S. Cho, Plasmonic-Enhanced Luminescence Characteristics of Microscale Phosphor Layers on a ZnO Nanorod-Arrayed Glass Substrate. *ACS Appl. Mater. Interfaces,* 2019, **11**, 1004−1012.
8. D. Lee, K. Yong, Superstrate $CuInS_2$ Photovoltaics with Enhanced Performance Using a CdS/ZnO Nanorod Array. *ACS Appl. Mater. Interfaces,* 2012, **4**, 6758−6765.
9. Y. Z. Gu, H. L. Lu, Y. Zhang, P. F. Wang, S. J. Ding, D. W. Zhang, Effects of ZnO Seed Layer Annealing Temperature on the Properties of n-ZnO NWs/Al_2O_3/p-Si Heterojunction. *Opt. Express,* 2015, **23**, 24457-24463.
10. B. Weintraub, Y. Deng, Z. L. Wang, Position-Controlled Seedless Growth of ZnO Nanorod Arrays on a Polymer Substrate via Wet Chemical Synthesis. *J. Phys. Chem.* C, 2007, **111**, 10162-10165.
11. T. Yasui, T. Yanagida, S. Ito, Y. Konakade, D. Takeshita, T. Naganawa, K. Nagashima, T. Shimada, N. Kaji, Y. Nakamura, I. A. Todorus, Y. He, S. Rahong, M. Kanai, H. Yukawa, T. Ochiya, T. Kawai, Y. Baba, Unveiling massive numbers of cancer-related urinary-microRNA candidates via nanowires, *Sci. Adv.* 2017, **3**, e1701133.
12. K. Shishino, T. Yamada, M. Arai, M. Ikeda, H. Hirata, M. Motoi, T. Hatakeyama, K. Teshima, A Strongly Adhering ZnO Crystal Layer via a Seed/buffer-Free, Low-Temperature Direct Growth on a Polyimide Film via a Solution Process. *CrystEngComm,* 2020, **22**, 5533–5538.
13. S. Vallejos, N. Pizurova, I. Gracia, C. S. Vazquez, J. Cechal, C. Blackman, I. Parkin, C. Cane, ZnO Rods with Exposed {100} Facets Grown via a Self-Catalyzed Vapor−Solid Mechanism and Their Photocatalytic and Gas Sensing Properties. *ACS Appl. Mater. Interfaces,* 2016, **8**, 33335−33342.

14. A. Jiamprasertboon, S. C. Dixon, S. Sathasivam, M. J. Powell, Y. Lu, T. Siritanon, C. J. Carmalt, Low-Cost One-Step Fabrication of Highly Conductive ZnO:Cl Transparent Thin Films with Tunable Photocatalytic Properties via Aerosol-Assisted Chemical Vapor Deposition. *ACS Appl. Electron. Mater*., 2019, **1**, 1408−1417.
15. J. d. Abajo, J. G. D. L. Campa, Processable Aromatic Polyimides. *Advances in Polymer Science,* 1999, **140**, 23-59.
16. J. Pei, J. Yang, T. Yildirim, H. Zhang, Y. Lu, Many-Body Complexes in 2D Semiconductors. *Adv. Mater.* 2019, **31**, 1706945
17. X. Jiang, A.V. Kuklin, A. Baev, Y. Ge, H. Agren, H. Zhang, P. N. Prasad, Two-dimensional MXenes: From morphological to optical, electric, and magnetic properties and applications. *Physics Reports,* 2020, **848**, 1-58
18. M. Zhang, Q. Wu, F. Zhang, L. Chen, X. Jin, Y. Hu, Z. Zheng, H. Zhang, 2D Black Phosphorus Saturable Absorbers for Ultrafast Photonics. *Adv. Optical Mater.* 2019, **7**, 1800224
19. S. Guo, Y. Zhang, Y. Ge, S. Zhang, H. Zeng, H. Zhang, 2D V-V Binary Materials: Status and Challenges. *Adv. Mater.* 2019, **31**, 1902352
20. M. Garg, J. K. Quamara, FTIR Analysis of High Energy Heavy Ion Irradiated Kapton-H Polyimide. *Indian J. Pure Appl. Phys*., 2007, **45**, 563-568.
21. L. E. Stephans, A. Myles, R. R. Thomas, Kinetics of Alkaline Hydrolysis of a Polyimide Surface. *Langmuir,* 2000, **16**, 4706-4710.
22. N. Inagaki, S. Tasaka, K. Hibi, Improved Adhesion between Plasma-Treated Polyimide Film and Evaporated Copper. *J. Adhesion Sci. Technol*., 1994, **8**, 395-410.
23. K. Akamatsu, S. Ikeda, H. Nawafune, Site-Selective Direct Silver Metallization on Surface-Modified Polyimide Layers. *Langmuir,* 2003, **19**, 10366-10371.
24. E.M. Bachari, G. Baud, S. B. Amor, M. Jacquet, Structural and optical properties of sputtered ZnO films. *Thin Solid Films,* 1999, **348**, 165-172
25. C. Pholnak, C. Sirisathitkul, S. Suwanboon, D. J. Harding, Effects of Precursor Concentration and Reaction Time on Sonochemically Synthesized ZnO Nanoparticles. *Mate. Res*., 2014, **17**, 405-411.
26. N. Uekawa, R. Yamashita, Y. J. Wu, K. Kakegawa, Effect of alkali metal hydroxide on formation processes of zinc oxide crystallites from aqueous solutions containing $Zn(OH)_4^{2-}$ ions. *Phys. Chem. Chem. Phys.,* 2004, **6**, 442-446